Ocean Sci. Discuss., 7, 391–415, 2010
www.ocean-sci-discuss.net/7/391/2010/

Ocean Science Discussions

This discussion paper is/has been under review for the journal Ocean Science (OS).
Please refer to the corresponding final paper in OS if available.

Anthropogenic carbon dynamics in the changing ocean

J. F. Tjiputra[1,2], **K. Assmann**[2], **and C. Heinze**[1,2]

[1]Geophysical Institute, University of Bergen Allégaten 70, 5007 Bergen, Norway
[2]Bjerknes Centre for Climate Research, Allégaten 55, 5007, Bergen, Norway

Received: 23 February 2010 – Accepted: 2 March 2010 – Published: 3 March 2010

Correspondence to: J. F. Tjiputra (jerry.tjiputra@bjerknes.uib.no)

Published by Copernicus Publications on behalf of the European Geosciences Union.

Abstract

Long-term response of CO_2 fluxes to climate change at the ocean surface and the ocean interior are investigated using a coupled climate-carbon cycle model. This study also presents the first attempt in quantifying the evolution of lateral transport of anthropogenic carbon under future climate change. Additionally, its impact on regional carbon storage and uptake are also evaluated. For the 1850–2100 period, our climate change simulation predicts oceanic uptake of anthropogenic carbon of about 538 Pg C. Another simulation indicates that changes in physical climate alone results in a release of natural carbon of about 22 Pg C. The natural carbon outgassing is attributed to the reduction in solubility and change in wind pattern in the Southern Hemisphere. After the anthropogenic carbon passes through the air-sea interface, it is predominantly transported along the large scale overturning circulation below the surface layer. The spatial variations in the transport patterns in turn influence the evolution of future regional carbon uptake. In the North Atlantic, a slow down in Atlantic Meridional Overturnning Circulation weakens the penetration strength of anthropogenic carbon into the deeper ocean, which leads to the reduced uptake rate in this region. In contrast, more than half of the anthropogenic carbon taken up in the high latitude Southern Ocean region (south of 58° S) are efficiently and continuously exported northward, predominantly into intermediate waters. This peculiar transport mechanism allow continuous increase in future carbon uptake in the high latitude Southern Ocean, where the annual uptake strength could reach 3.5 g C m^{-2} yr^{-1}, nearly triple the global mean of 1.3 g C m^{-2} yr^{-1} by the end of the 21st century. Our study further underlines the key role of the Southern Ocean in controlling long-term future carbon uptake.

1 Introduction

The world ocean is a major sink for the anthropogenic carbon emitted since 1750 (Sabine et al., 2004; Le Quéré et al., 2009). Air-sea carbon fluxes depend on phys-

ical, chemical, and biological processes. They change with increasing atmospheric CO_2 concentrations in a complex adjustment process. Climate change resulting from higher atmospheric CO_2 concentration induces different feedback mechanisms that could further complicate the prediction of future strength and distribution of oceanic carbon sinks.

A historically important climate-carbon cycle feedback is the variability of the ocean circulation associated with past climate change. This feedback had been shown to play a major role in controlling the distribution of deep ocean carbon storage, and therefore the regional air-sea CO_2 fluxes (Wallace, 2001; Olsen et al., 2006; Takahashi et al., 2006; Toggweiler et al., 2006; Watson and Naveira-Garabato, 2006; Smith et al., 2008; Thomas et al., 2008; Cao et al., 2009). Understanding how current and future climate variability affects the time-evolving ocean circulation and the associated distribution of deep ocean carbon is important to understand future net air-sea CO_2 fluxes.

In previous years, several studies have estimated the lateral transport of carbon in different ocean regions (Stoll et al., 1996; Holfort et al., 1998; Álvarez et al., 2003; Macdonald et al., 2003; Mikaloff Fletcher et al., 2006; Gruber et al., 2009; Ito et al., 2010). These studies in general were limited by the consideration of fixed present-day internal oceanic carbon transport rates. They thus neglected the potential change or carbon transport rates in response to anthropogenic climate change. Currently, an Earth system model is the only tool that can simulate the complex interactions and long-term feedback effects between the global climate and carbon cycle. In this study, we apply such a model to quantitatively estimate the long-term response of oceanic carbon fluxes, transports, and storage. In addition, the implication of regional transport and storage variability on the future regional air-sea CO_2 fluxes and inventories will be determined.

2 Experimental design

Here, we use the Bergen Earth system model (BCM-C) (Tjiputra et al., 2010), which is based on the extension of Bergen Climate Model (Furevik et al., 2003; Ottera et al., 2009). The atmosphere component is the spectral atmospheric general circulation model ARPEGE from the Meteo-France. The physical ocean component is based on the Miami Isopycnic Coordinate Ocean Model (MICOM). For the carbon cycle interactions, the Lund-Potsdam-Jena (LPJ) represents the terrestrial biosphere and the marine carbon cycle is represented by the Hamburg Ocean Carbon Cycle model (HAMOCC5.1). The marine biogeochemical model HAMOCC5.1 was adopted for use in the isopycnal physical ocean model MICOM (Assmann et al., 2010). The horizontal rezolution of the model is approximately 2.8°×2.8°. More detailed description of the model components are available in Tjiputra et al. (2010).

The BCM-C is applied in three multi-century simulations for the period of 1850–2099 (see Table 1): (1) "EXP1", where all physical and atmospheric CO_2 forcings are held at preindustrial level (PRE, i.e., constant 284.7 ppmv), (2) "EXP2", with interactive climate and carbon cycle evolution based on prescribed historical and the SRES-A2 CO_2 emissions scenario (Marland et al., 2005; Houghton and Hackler, 2002), and finally (3) "EXP3", where the climate varies according to atmospheric CO_2 from EXP2 (i.e., the atmospheric and oceanic circulation are identical to EXP2) but the ocean and terrestrial carbon cycle interact with preindustrial CO_2 concentration.

The experiment is thus designed that the difference between EXP3 and EXP1 represents the changes in natural carbon (C_{nat}) as a result of climate change, whereas the difference between EXP2 and EXP3 represents the response of anthropogenic carbon (C_{ant}) under the projected future climate change.

For the analysis, we compute the regional and temporal variations of C_{nat} and C_{ant} uptake at the air-sea interface. In addition, the lateral transports of C_{ant} within different ocean basins are quantified. For each latitude, the meridional carbon transport is computed by summing up the net northward dissolved inorganic carbon (DIC) transport

over all vertical layers:

$$\Psi_{CO_2}(j,t) = \int_x \int_z C \cdot V \, dz \, dx. \quad (1)$$

where j represents latitudes, t represents time, and x, z represent the zonal and vertical distribution of model grid points. Here, C and V are the prognostic DIC concentration and the net northward volume transport leaving the grid cell, respectively. Thus, the meridional anthropogenic carbon transport, for example C_{ant} at a specific latitude and time, is simply the difference of computed Ψ_{CO_2} between EXP2 and EXP3. Note that the model simulates a reasonable range of present-day maximum Atlantic Meridional Overturning Circulation (AMOC) strength of 19–22 Sv, consistent with a multi-GCMs study (Schmittner et al., 2005).

3 Model validation

The model captures the general characteristics of observed climate variability. It also simulates realistically the large scale structure of the global ocean stream fuction (Furevik et al., 2003). The simulated climate change and carbon fluxes are well within range of other earth system models (Friedlingstein et al., 2006; Tjiputra et al., 2010). In the simulation of the 1990s, the annual mean anthropogenic carbon uptake across the air-sea interface is 2.35±0.2 Pg C yr^{-1}, well within the range of independent estimates from inversion study of 2.2±0.25 Pg C yr^{-1} (Mikaloff Fletcher et al., 2006) as well as recently published pCO_2 climatology-based estimates (Takahashi et al., 2009) of 1.6±0.9 Pg C yr^{-1}. The model also reproduces well the observed estimates of the large-scale distribution of air-sea carbon fluxes. Regions of mean outgassing comprise the familiar upwelling regions such as the tropical regions, with strongest outflux in the eastern Equatorial Pacific. Uptake regions are simulated in the temperate regions between 30° and 60° lattitudes of both hemispheres. For the Antarctic polar region (south of 58° S), the BCM-C simulates a contemporary net carbon sink of 0.25±0.04 Pg C yr^{-1}.

For the same region, an observation-based study suggests a net carbon source of 0.04 Pg C yr^{-1} (Takahashi et al., 2009), whereas inversion study suggests a similar sink of ~0.2±0.1 Pg C yr^{-1} (Mikaloff Fletcher et al., 2006, 2007).

The accumulated global anthropogenic carbon uptake for the period from 1850–1999 is 106.5±12.5 Pg C. During this period, more than 48% of the atnhropogenic carbon uptake through the air-sea interface occurs in the Southern Ocean (south of 18° S). The greatest per-unit-area uptake occurs in the North Atlantic (18° N–66° N) region, where it is responsible for nearly 13% of the total uptake, despite representing only 8% of the world ocean area. As expected, the equatorial regions take up least anthropogenic carbon. These spatial variations in anthropogenic CO_2 uptake across different regions are generally in good agreement with estimates from other study (Sabine et al., 2004; Gerber et al., 2009; Vázquez-Rodríguez et al., 2009). A more complete evaluation of the model's performance and validation is also discussed in Tjiputra et al. (2010).

We acknowledge limitations within the BCM-C model. For example, due to the nature of the fully coupled earth system model, the simulated temporal variabilities in the air-sea CO_2 fluxes are not directly comparable with the recently-reported variabilities in the Southern Ocean (Le Quéré et al., 2007), North Atlantic (Schuster and Watson, 2007), Tropical Pacific (Feely et al., 2006), and North Pacific (Takahashi et al., 2006; Keeling et al., 2004), although the internal variability simulated by the model is realistic in a statistical sense.

4 Results

4.1 Changes in natural carbon fluxes across the air-sea interface

Understanding the interplay mechanisms between natural and anthropogenic carbon is essential in predicting future oceanic uptake. Several studies have indicated that the long-term balance of C_{nat} fluxes will be altered in the future due to climate change (Le Quéré et al., 2007; Zickfeld et al., 2007). Here, the response of C_{nat} fluxes accross

the air-sea interface to future climate perturbation are estimated by differencing the results from EXP1 and EXP3. For the 1850–2100 period, the time-integrated C_{nat} fluxes amount to about 22 Pg C outgassing.

Figure 1 shows that the main C_{nat} outgassing regions are located in the tropical and mid-latitude regions and most of the Southern Ocean. We attribute part of the future outgassing of C_{nat} to SST warming, which resulted in reduction of gas solubility in seawater accross all latitudes (see Fig. 1b).

Figure 1c also shows that our climate change simulation also indicates a strengthening and poleward shift (i.e., approximately 40° S to 45° S, see also supplemental Fig. 1, http://www.ocean-sci-discuss.net/7/391/2010/osd-7-391-2010-supplement.pdf) in the Southern Ocean surface wind speed, consistent with previous studies (Fyfe and Saenko, 2006; Zickfeld et al., 2007). In their study (Zickfeld et al., 2007), similar changes in the Southern Hemisphere winds leads to increased upwelling of DIC-rich waters and hence ventilation of C_{nat} south of 55° S. In our model, the 40° S latitude band represents a mean influx of C_{nat} into the ocean. Therefore, the poleward wind shift weakens the gas transfer rate across most of this latitudinal band, which results in reduced uptake strength of the C_{nat} (i.e., a global net outgassing).

While the study by Zickfeld et al. (2007) also resulted in net outgassing of natural carbon, it is important to note that the mechanism that acting in their model is slightly different as compared to this study, despite a similar poleward wind shift perturbation. These discrepancies can be attributed to the spatial difference in the air-sea CO_2 fluxes simulated by the two models. In addition to the zonal wind shift in our climate change simulation, a substantial retreat of sea-ice in the southern polar latitude (shown in Fig. 1d) leads to an additional uptake of C_{nat} (see also Tjiputra et al., 2010).

4.2 Anthropogenic carbon uptake and storage

The accumulated air-sea uptake of C_{ant} during the 1850–2099 period amounts to about 538 Pg C. Most of this uptake is confined to the dominant C_{ant} uptake regions similar to the present day. These regions include the North Atlantic sub-polar gyre, northwestern

Pacific, Equatorial Pacific, and most of the Southern Ocean (south of 30° S), as shown in Fig. 2a. Once the anthropogenic carbon passes through the air-sea interface, it is predominantly transported along the large scale overturning circulation below the surface layer. This circulation, in turn controls the future distribution of C_{ant} in the deep ocean. Figure 2 illustrates that C_{ant} is not necessarily stored in the region where it is taken up by the ocean and highlights the role of C_{ant} lateral transport in the ocean interior.

Figure 2c shows substantial uptake of C_{ant} between 30° S and 65° S, a considerable amount of which is subsequently stored outside this region. This high-uptake-low-inventory feature in the high latitude Southern Ocean region is consistent with recent observations and modeling studies (Caldeira and Duffy, 2000; Sabine et al., 2004; Ito et al., 2010). In the Northern Hemisphere, there is a net influx of subsurface C_{ant} into the northern mid-latitude regions (i.e., between 10° N and 50° N). To better undertand the role of lateral transport below the surface layer, in the next subsection, we attempt to quantify the regional and temporal evolution of C_{ant} transport.

4.3 Anthropogenic carbon transport

To analyze the large scale response of anthropogenic carbon lateral transport across different ocean basins, we compute the latitudinal meridional mass transport of C_{ant} following Eq. (1). Figure 3 summarizes the simulated mean-decadal meridional migration of anthropogenic carbon across different ocean sections for the period 1850–2099 together with available modern observation-based estimates as well as results from previous modeling studies.

For the early anthropocene period, there is a weak and consistent meridional transport of C_{ant}, northward within both the Atlantic and Pacific, and southward in the Indian Ocean. In the Atlantic Ocean, the northward C_{ant} transports range from negligible amounts in the Northern Hemisphere to 0.02 Pg C yr^{-1} in the Southern Hemisphere. The northward conveyance is due to the fact that the upper ocean waters of the Atlantic Ocean, where most of the anthropogenic CO_2 resides, moves predominantly

northward.

Meridional transport in the Pacific Ocean occurs mostly with a similar magnitude. Near the equator, the meridional transport is very close to zero, suggesting dominant westward transport of C_{ant} passing the Indonesian archipelago into the Indian Ocean. Consequently, the meridional transport of C_{ant} in the Indian Ocean is uniformly southward with increasing magnitudes toward its southern extent.

Figure 3 also shows that the model simulates an increasing strength of the meridional C_{ant} transport as compared to the preindustrial period in most regions. This is expected as the ocean is continuously taking up further C_{ant}. For modern conditions (i.e., 1990s, solid black line in Fig. 3), the northward transport in the Atlantic Ocean increases significantly to nearly 0.2 Pg C yr^{-1} for the region south of 15° N, and decreases toward the Arctic. Simulated northward C_{ant} transports for the region south of 15° N are in general agreement with independent estimates. Estimates from both data assimilation and inverse studies (Mikaloff Fletcher et al., 2006; Gerber et al., 2009; Gruber et al., 2009) suggest a similar pattern of northward transport of C_{ant} in the Atlantic Ocean that is maximized in the Southern Hemisphere. An observation-based study (Holfort et al., 1998) suggests northward transport (0.11±0.03–0.26±0.03 Pg C yr^{-1}) in the region between 11° S and 30° S. Previous studies have offered considerably diverging estimates of modern northward transport strength across the 24.5° N: 0.24±0.04 Pg C yr^{-1} (Álvarez et al., 2003), 0.19±0.07 Pg C yr^{-1} (Macdonald et al., 2003), and about 0.08 Pg C yr^{-1} (Gruber et al., 2009). Our estimates are in the centre of that range, 0.15±0.04 Pg C yr^{-1}. Disagreements can be attributed to spatial variation in the carbon uptake estimates and the large month-to-month variation in the observed meridional overturning circulation strength (Cunningham et al., 2007). In the high latitude North Atlantic, our estimates are in good agreement with other studies as shown in Fig. 3.

In the Pacific, our modern day C_{ant} transport estimate also lie around the centre of an inverse study and data-based estimates. The model simulates maximum northward transport of 0.15 Pg C yr^{-1} in the South Pacific and relatively weak northward transport

in the North Pacific. In the Equatorial Pacific, the model simulates almost no meridional conveyance, indicating westward transport toward the Indian Ocean.

In the Indian Ocean, our modern transport estimates agree well with the inversion study (Mikaloff Fletcher et al., 2006), with 0.15 Pg C yr^{-1} southward transport in the Southern Hemisphere and small lateral transport north of 8° S. The former transport pattern is consistent with the zonal transport in the near-equatorial Pacific region, which carries C_{ant} passing the Indonesian throughflow into the Indian Ocean. The data assimilation study by Gerber et al. (2009) assumed zero net transport across the Indonesian throughflow, which resulted in large discrepancies with our transport estimates accross the South Pacific and South Indian sections. In the Indian Ocean, southward transport patterns are also consistent with observation based estimates (Sabine et al., 1999), which reported maximum anthropogenic CO_2 concentrations south of 30° S.

By the end of the 21st century, the latitudinal gradient in meridional anthropogenic carbon transport becomes more apparent. In the Atlantic, there is a net northward transport of anthropogenic carbon, with the greatest amplitude (0.65 Pg C yr^{-1}) in the southern portion. In the northern portion, the northward transport is weaker, which could be attributed to the horizontal and vertical return flows associated with the overturning circulation. This negative gradient in latitudinal transport of anthropogenic carbon in the Atlantic basin resulted in large amount of anthropogenic carbon (101.2 Pg C) stored in the northern regions between 18° N–66° N by the end of this century (see also Figs. 2c and 4).

The northward transport of C_{ant} from the Southern Ocean into the Pacific Ocean also increases significantly (0.65 Pg C yr^{-1}) toward the end of the model simulation. This northward flux is approximately offset by the southward transport from the Indian Ocean into the Southern Ocean, which resulted in relatively small net gain (i.e., in the mid-latitude Southern Ocean) in carbon storage due to lateral transport from both the Pacific and Indian Oceans.

5 Discussion

In this section we discuss some implication of the C_{ant} transport variations for the future uptake and storage of anthropogenic carbon. Figure 4 shows a large-scale overview of future time-integrated transport and inventory of anthropogenic carbon. It quantitatively illustrates the long-term accumulation of anthropogenic carbon due to the combined effects of air-sea gas exchange and lateral transport for the period of 1850–2099 and for different ocean basins.

By the end of the century, in the Indian Ocean, the C_{ant} invetory is roughly equal to the anthropogenic carbon uptake through the air-sea interface, since there are nearly equal lateral inflow (from the Indonesian throughflow) and lateral outflow (to the Southern Ocean) rates of anthropogenic carbon into and out of this region.

The model simulation shows that the Equatorial Pacific is one of the only two regions (the high latitude Southern Ocean is the other) having a net C_{ant} outflow. This is reflected by more C_{ant} transported into the Indian (-44.6 Pg C) and North Pacific (-18 Pg C) as compared to input from Southern Ocean (37.4 Pg C). Here, the Indonesian throughflow is an important mechanism in transporting most of the C_{ant} taken up across the air-sea interface (in the Equatorial Pacific) to the Indian Ocean. A smaller portion of C_{ant} is transported northward to the North Pacific.

Both the North Pacific and North Atlantic Oceans exhibit similar C_{ant} flux patterns. This is intriguing despite the fact that both the North Pacific and the North Atlantic are on the opposite ends of the global meridional overturning circulation. While most of the C_{ant} inventory in these regions originates directly from the atmosphere, considerable amounts are imported from the southern portion of the respective ocean basins. Additionally, in the North Atlantic, the simulated climate change leads to a weakening of the Atlantic Meridional Overturning Circulation (AMOC) strength by approximately 7 Sv. Since deep water formation associated with AMOC is the principal mechanism for transporting C_{ant} from surface to the deep ocean (e.g., in the North Atlantic), the weakening leads to weaker penetration of C_{ant} into deeper layers. These mechanisms

(i.e., influx of near surface of C_{ant} from the south and reduced export strength) could alter the atmospheric C_{ant} uptake strength in the North Atlantic.

In the Arctic, approximately equal amounts of the accumulated C_{ant} (7.3 Pg C) in the region come from the lateral transport and through the air-sea interface. Our transport estimates in the region are consistent with an earlier study (Lundberg and Haugan, 1996), which indicates that the total carbon flux to the Nordic Seas and Arctic Ocean is dominated by the influx from the Bering Strait.

By the end of the century, the largest time-integrated (1850–2099) C_{ant} uptake from the atmosphere, about 180 Pg C, occurs in the Southern Ocean, between 18° S–58° S. In addition, there are accumulated inflows of 44.0 and 43.9 Pg C from the Indian and high latitude Southern Oceans, and outflows of 37.4 and 45.5 Pg C into the Pacific and Atlantic Oceans, respectively. These lateral fluxes combine for a net influx of only 5 Pg of C_{ant} over the experiment period, and make the Southern Ocean (18° S–58° S) the dominant region for C_{ant} storage with 191.5 Pg C.

Finally, the high latitude Southern Ocean region (SOC2 in Fig. 4) appears to be the only region with significant and continuous uptake and outflow of anthropogenic carbon. Figure 4 illustrates that approximately half of the C_{ant} absorbed in this region is subsequently transported into regions further north. This northward anthropogenic carbon transport mostly occurs along the subduction of the intermediate water masses with maximum conveyance at approximately 400–500 m depth. A similar mechanism is hyphothesized for the present day condition (Caldeira and Duffy, 2000; Gerber et al., 2009; Gruber et al., 2009; Vázquez-Rodríguez et al., 2009; Ito et al., 2010). Our model simulation demonstrates that this C_{ant} export pattern is robust and will continue toward the end of the 21st century. In the model, the opening of sea ice also contributes to the increase in C_{ant} uptake across the air-sea interface in the region.

To link the potential role of regional lateral transport with the future C_{ant} uptake, we compute the evolution of regional C_{ant} uptakes for the same ocean regions discussed above, as illustrated in Fig. 5. For the present day period, the highest anthropogenic carbon uptake occurs in the North Atlantic and high latitude Southern Ocean. By the

OSD
7, 391–415, 2010

end of the century, the anthropogenic carbon uptake appears to stabilize in most ocean regions. However, the uptake rate in the high latitude Southern Ocean continues to increase further. This is consistent with our previous transport analysis, which indicates efficient transport of C_{ant} out of the high latitude Southern Ocean into deepwater areas further north. In addition, Fig. 5 also shows stabilization of C_{ant} uptake in the North Atlantic and North Pacific, which can partly be attributed to the significant lateral influx of C_{ant} into the regions. We also note that the stabilization of anthropogenic carbon uptake in most ocean regions is partly attributed to the the long-term equilibration time for atmospheric CO_2 into the ocean (Archer et al, 2009).

By the end of the century, the global ocean has taken up 537 Pg of C_{ant} in our simulation. Large portions of this amount reside in the Southern Ocean (between 18° S and 58° S), 191.5 Pg C, and the North Atlantic Ocean (between 18° N and 66° N), 101 Pg C. Both regions combine account for 55% of the global inventory.

6 Conclusions

Recently, Earth system models have been employed to analyze the potential vulnerabilities of future ocean carbon uptake due to changes in the climate system, such as temperature and atmospheric circulation (Friedlingstein et al., 2006; Crueger et al., 2008). In this study, we applied the Bergen Earth system model to analyze the role of ocean circulation in controlling future distribution of oceanic anthropogenic CO_2 concentration and its potential implication on future air-sea CO_2 fluxes.

For the period of 1850–2099, outgassing of natural carbon is simulated in our model, which amounts to a total of 22 Pg C. The accumulated uptake of anthropogenic carbon for the same period amounts to about 538 Pg C. Our model study thus implies that feedbacks from climate change induced circulation and other physical changes do not reduce the ocean's ability in taking up anthropogenic carbon substantially.

Here, we determine the role of the ocean circulation in transporting the absorbed anthropogenic carbon, and the implications on the regional carbon uptake in the fu-

ture. Our study shows that the ability of the high latitude Southern Ocean region (i.e., south of 58° S) to take up anthropogenic CO_2 will continue to increase in the future, in contrast to other regions which see reduction or stabilization of anthropogenic carbon uptake. We also would like to stress the still considerable uncertainties about Southern Ocean carbon cycling and its variations due to climate change. Lateral transports of anthropogenic carbon in most other regions (i.e., tropical regions) prominently occur within the surface or near-surface level. Therefore, they generally do not provide efficient deepwater pathways for export of anthropogenic carbon.

In the North Atlantic, despite the high uptake rate across the air-sea interface, a substantial amount of subsurface anthropogenic carbon is transported into the region (i.e., from the tropics). This northward transport has already altered the carbon uptake rate in regions such as the Nordic Seas (Olsen et al., 2006). A continuous inflow of CO_2-rich near-surface water may potentially contribute to the stabilization of carbon uptake in the North Atlantic Ocean in the future (see also Fig. 5).

All of the available observation-based estimates of anthropogenic carbon transport have been conducted in the Atlantic Ocean so far. Future observations in the Pacific and Indian Oceans would undoubtfully be useful to constrain future prediction of climate change associated carbon transport.

Acknowledgements. The authors thank Are Olsen and Justin Wettstein for the constructive feedbacks on this manuscript. This study at the University of Bergen and Bjerknes Centre for Climate Research is supported by the EU-FP6 integrated project CarboOcean (grant no. 511176), the Research Council of Norway funded project NorClim and CarboSeason (grant no. 1805/530). The experiments in this study is also made possible through the supercomputing support from NOTUR (Norwegian Metacenter for Computational Science), biogeochemical earth system modelling project (no. nn2980k) and the respective archiving project NorStore (Norwegian Storage Infrastructure) (no. ns2980k).

References

Álvarez, M., Ríos, A. F., Pérez, F. F., Bryden, H. L., and Rosón, G.: Transports and budgets of total inorganic carbon in the subpolar and temperate North Atlantic, Global Biogeochem. Cy., 17(1), 1002, doi:10.1029/2002GB001881, 2003. 393, 399, 413

Archer, D., Eby, M., Brovkin, V., Ridgwell, A., Cao, L., Mikolajewicz, U., Caldeira, K., Matsumoto, K., Munhoven, G., Montenegro, A., and Tokos, K.: Atmospheric lifetime of fossil fuel carbon dioxide, Ann. Rev. Earth Planet Sci., 37, 117–134, 2009. 403

Assmann, K. M., Bentsen, M., Segschneider, J., and Heinze, C.: An isopycnic ocean carbon cycle model, Geosci. Model Dev., 3, 143–167, 2010. 394

Caldeira, K. and Duffy, P. B.: The role of the Southern Ocean in the uptake and storage of anthropogenic carbon dioxide, Science, 287, 620–622, 2000. 398, 402

Cao, L., Eby, M., Ridgwell, A., Caldeira, K., Archer, D., Ishida, A., Joos, F., Matsumoto, K., Mikolajewicz, U., Mouchet, A., Orr, J. C., Plattner, G.-K., Schlitzer, R., Tokos, K., Totterdell, I., Tschumi, T., Yamanaka, Y., and Yool, A.: The role of ocean transport in the uptake of anthropogenic CO_2, Biogeosciences, 6, 375–390, 2009, http://www.biogeosciences.net/6/375/2009/. 393

Crueger, T., Roeckner, E., Raddatz, T., Schnur, R., and Wetzel, P.:Ocean dynamics determine the response of oceanic CO_2 uptake to climate change, Clim. Dynam., 31, 151–168, doi:10.1007/s00382-007-0342-x, 2008. 403

Cunningham, S. A., Kanzow, T., Rayner, D., Baringer, M. O., Johns, W. E., Marotzke, J., Longworth, H. R., Grant, E. M., Hirschi, J. J.-M., Beal, L. M., Meinen, C. S., and Briden, H. L.: Temporal variability of of the Atlantic meridional overturning circulation at 26.5° N, Science, 317(5840), 935–938, doi:10.1126/science.1141304, 2007. 399

Feely, R., Takahashi, T., Wanninkhof, R., McPhaden, M. J., Cosca, C. E., Sutherland, S. C., and Carr, M.-E., J. Geophy. Res., 111, C08S90, doi:10.1029/2005JC003129, 2006. 396

Friedlingstein, P., Cox, P., Betts, R., Bopp, L., von Bloh, W., Brovkin, V., Cadule, P., Doney, S., Eby, M., Fung, I., Gala, B., John, J., Jones, C., Joos, F., Kato, T., Kawamiya, M., Knorr, W., Lindsay, K., Matthews, H. D., Raddatz, T., Rayner, P., Reick, C., Roeckner, E., Schnitzler, K.-G., Schnur, R., Strassmann, K., Weaver, A. J., Yoshikawa, C., and Zeng, N.: Climate–carbon cycle feedback analysis: Results from the C^4MIP model intercomparison, J. Climate, 19, 3337–3353, 2006. 395, 403

Furevik, T., Bentsen, M., Drange, H., Kindem, I. K. T., Kvamstø, N. G., and Sorteberg, A.:

Description and evaluation of the bergen climate model: ARPEGE coupled with MICOM, Clim. Dynam., 21, 27–51, doi:10.1007/s00382-003-0317-5, 2003. 394, 395

Fyfe, J. C. and Saenko, O. A.: Simulated changes in the extratropical Southern Hemisphere winds and currents, Geophys. Res. Lett., 33, L06701, doi:10.1029/2005GL025332, 2006. 397

Gerber, N., Joos, F., Vázquez-Rodríguez, M., Touratier, F., and Goyet, C.: Regional air-sea fluxes of anthropogenic carbon inferred with an Ensemble Kalman Filter, Global Biogeochem. Cy., 23, GB1013, doi:10.1029/2008GB003247, 2009. 396, 399, 400, 402, 413

Gruber, N., Gloor, M., Mikaloff Fletcher, S. E., Doney, S. C., Dutkiewicz, S., Follows, M. J., Gerber, M., Jacobson, A. R., Joos, F., Lindsay, K., Menemenlis, D., Mouchet, A., Müller, S. A., Sarmiento, J. L., and Takahashi, T.: Oceanic sources, sinks, and transport of atmospheric CO_2, Global Biogeochem. Cy., 23, GB1005, doi:10.1029/2008GB003349, 2009. 393, 399, 402, 413

Holfort, J., Johnson, K. M., Schneider, B., Siedler, G., and Wallace, D. W. R.: Meridional transport of dissolved inorganic carbon in the South Atlantic Ocean, Global Biogeochem. Cy., 12, 479–499, 1998. 393, 399, 413

Houghton, R. A. and Hackler, J. L.: Carbon flux to the atmosphere from land-use changes. Trends: A compendium of data on global change, Carbon Dioxide Information Analysis Center, US Department of Energy, Oak Ridge, TN, USA, 2002. 394

Ito, T., Woloszyn, M., and Mazloff, M: Anthropogenic carbon dioxide transport in the Southern Ocean driven by Ekman flow, Nature, 473, 80–83, doi:10.1038/nature08687, 2010. 393, 398, 402

Keeling, C., Brix, H., and Gruber, N.: Seasonal and long-term dynamics of the upper ocean carbon cycle at station ALOHA near Hawaii, Global Biogeochem. Cy., 18, GB4006, doi:10.1029/2004GB002227, 2004. 396

Le Quéré, C., Rödenbeck, C., Buitenhuis, E. T., Conway, T. J., Langenfelds, R., Gomez, A., Labuschagne, C., Ramonet, M., Nakazawa, T., Metzl, N., Gillett, N., and Heimann, M.: Saturation of the Southern Ocean CO_2 sink due to recent climate change, Science, 316, 1735–1738, 2007. 396

Le Quéré, C., Raupach, M. R., Canadell, J. G., Marland, G., Bopp, L., Ciais, P., Conway, T. J., Doney, S. C., Feely, R. A., Foster, P., Friedlingstein, P., Gurney, K., Houghton, R., A., House, J. I., Huntingford, C., Levy, P. E., Lomas, M. R., Majkut, J., Metzl, N., Ometto, J. P., Peters, G. P., Prentice, I. C., Randerson, J. T., Running, S. W., Sarmiento, J. L., Schuster, U., Sitch,

S., Takahashi, T., Viovy, N., van der Werf, G. R., and Woodward, F. I.: Trends in the sources and sinks of carbon dioxide, Nature Geosci., 2, 831–836, doi:10.10.1038/NGEO789, 2009. 392

Lefèvre, N., Watson, A. J., Olsen, A., Rios, A. F., Perez, F. F., and Johannessen, T.: A decrease in the sink for atmospheric CO_2 in the North Atlantic, Geophys. Res. Lett., 31, L07306, doi:10.1029/2003GL018957, 2004.

Lenton, A., Codron, F., Bopp, L., Metzl, N., Cadule, P., Tagliabue, A., and Le Sommer, J.: Stratospheric ozone depletion reduces ocean carbon uptake and enhances ocean acidification, Geophys. Res. Lett., 36, L12606, doi:10.1029/2009GL038227, 2009.

Lovenduski, N. S., Gruber, N., and Doney, S. C.: Toward a mechanistic understanding of the decadal trends in the Southern Ocean carbon sink, Global Biogeochem. Cy., 22, GB3016, doi:10.1029/2007GB003139, 2008.

Lunberg, L. and Haugan, P.: A Nordic Seas–Arctic Ocean carbon budget from volume flows and inorganic carbon data, Global Biogeochem. Cy., 10, 493–510, 1996. 402

Marinov, I., Gnanadesikan, A., Toggweiler, J. R., and Sarmiento, J. L.: The Southern Ocean biogeochemical divide, Nature, 441, 964–967, doi:10.1038/nature04883, 2006.

Marland, G., Boden, T. A., and Andres, R. J.: Global, regional, and national CO_2 emissions. Trends: A compendium of data on global change, Carbon Dioxide Information Analysis Center, US Department of Energy, Oak Ridge, TN, USA, 2005. 394

Macdonald, A. M., Baringer, M. O., Wanninkhof, R., Lee, K., and Wallace, D. W. R.: A 1998–1002 comparison of inorganic carbon and its transport across 24.5° N in the Atlantic, Deep Sea Res. II, 50(22–26), 3041–3064, doi:10.1016/j.dsr2.2003.07.009, 2003. 393, 399, 413

Mikaloff Fletcher, S. E., Gruber, N., Jacobson, A. R., Doney, S. C., Dutkiewicz, S., Gerber, M., Follows, M., Joos, F., Lindsay, K., Menemenlis, D., Mouchet, A., Müller, S. A., and Sarmiento, J. L.: Inverse estimates of anthropogenic CO_2 uptake, transport, and storage by the ocean, Global Biogeochem. Cy., 20, GB2002, doi:10.1029/2005GB002530, 2006. 393, 395, 396, 399, 400, 413

Mikaloff Fletcher, S. E., Gruber, N., Jacobson, A. R., Gloor, M., Doney, S. C., Dutkiewicz, S., Gerber, M., Follows, M., Joos, F., Lindsay, K., Menemenlis, D., Mouchet, A., Müller, S. A., and Sarmiento, J. L.: Inverse estimates of the oceanic sources and sinks of natural CO_2 and the implied oceanic carbon transport, Global Biogeochem. Cy., 21, GB1010, doi:10.1029/2006GB002751, 2007. 396

Otterá, O. H., Bentsen, M., Bethke, I., and Kvamstø, N. G.: Simulated pre-industrial climate

in Bergen Climate model (version 2): Model description and large-scale circulation features, Geosci. Model Dev., 2, 197–212, 2009. 394

Olsen, A., Omar, A. M., Bellerby, R. G. J., Johannessen, T., Ninnemann, U., Brown, K., Olsson, A., Olafsson, J., Nondal, G., Kivimäe, C., Kringstad, S., Neill, C., and Olafsdottir, S.: Magnitude and origin of the anthropogenic CO_2 increase and ^{13}C Suess effect in the Nordic seas since 1981, Global Biogeochem. Cy., 20, GB3027, doi:10.1029/2005GB002669, 2006. 393, 404

Sabine, C. L., Key, R. M., Johnson, K. M., Millero, F. J., Poisson, A., Sarmiento, J. L., Wallace, D. W. R., and Winn, C. D.: Anthropogenic CO_2 inventory of the Indian Ocean, Global Biogeochem. Cy., 13, 179–198, 1999. 400

Sabine, C. L., Feely, R. A., Gruber, N., Key, R. M., Lee, K., Bullister, J. L., Wanninkhof, R., Wong, C. S., Wallace, D. W. R., Tilbrook, B., Millero, F. J., Peng, T.-H., Kozyr, A., Ono, T., and Rios, A. F.: The oceanic sink for anthropogenic CO_2, Science, 305, 367–371, 2004. 392, 396, 398

Schmittner, A., Latif, M., and Schneider, B.: Model projections of the North Atlantic thermohaline circulation for the 21st century assessed by observations, Geophys. Res. Lett., 32, L23710, doi:10.1029/2005GL024368, 2005. 395

Schuster, U. and Watson, A. J.: A variable and decreasing sink for atmospheric CO_2 in the North Atlantic, J. Geophys. Res., 112, C11006, doi:10.1029/2006JC003941, 2007. 396

Smith, R. S. and Marotzke, J.: Factors influencing anthropogenic carbon dioxide uptake in the North Atlantic in models of the ocean carbon cycle, Clim. Dynam., 31, 599–613, 2008. 393

Stoll, M. H. C., van Aken, H. M., de Baar, H. J. W., and de Boer, C. J.: Meridional carbon dioxide transport in the northern North Atlantic, Mar. Chem., 55, 205–216, 1996. 393

Takahashi, T., Sutherland, S. C., Feely, R. A., and Cosca, C. E.: Decadal variation of the surface water pCO_2 in the western and eastern equatorial Pacific, Science, 302, 852–856, 2003.

Takahashi, T., Sutherland, S. C., Feely, R. A., and Wanninkhof, R.: Decadal change of the surface water pCO_2 in the North Pacific: A synthesis of 35 years of observations, J. Geophys. Res., 111, C07S05, doi:10.1029/2005JC003074, 2006. 393, 396

Takahashi, T., Sutherland, S. C., Wanninkhof, R., Sweeney, C., Feely, R. A., Chipman, D. W., Hales, B., Friedrich, G., Chavez, F., Sabine, C., Watson, A., Bakker, D. C. E., Schuster, U., Metzl, N., Yoshikawa-Inoue, H., Ishii, M., Midorikawa, T., Nojiri, Y., Körtzinger, A., Steinhoff, T., Hoppema, M., Olafsson, J., Arnarson, T. S., Tilbrook, B., Johannessen, T., Olsen, A., Bellerby, R., Wong, C. S., Delille, B., Bates, N. R., and de Baar, H. J. W.: Climatological

mean and decadal change in surface ocean pCO_2, and net sea-air CO_2 flux over the global oceans, Deep Sea Res. II, 56, 554–577, 2009. 395, 396

Thomas, H., Friederike Prowe, A. E., Lima, I. D., Doney, S. C., Wanninkhof, R., Greatbatch, R. J., Schuster, U., and Corbière, A.: Changes in the North Atlantic Oscillation influence CO_2 uptake in the North Atlantic over the past 2 decades, Global Biogeochem. Cy., 22, GB4027, doi:10.1029/2007GB003167, 2008. 393

Toggweiler, J. R., Russell, J. L., and Carson, S. R.: Midlatitude westerlies, atmospheric CO_2, and climate change during the ice ages, Paleoceanography, 21, PA2005, doi:10.1029/2005PA00154, 2006. 393

Tjiputra, J. F., Assmann, K., Bentsen, M., Bethke, I., Otterå, O. H., Sturm, C., and Heinze, C.: Bergen earth system model (BCM-C): Model description and regional climate–carbon cycle feedbacks assessment, Geosci. Model Dev., 3, 123–167, 2010. 394, 395, 396, 397

Vázquez-Rodríguez, M., Touratier, F., Lo Monaco, C., Waugh, D. W., Padin, X. A., Bellerby, R. G. J., Goyet, C., Metzl, N., Ríos, A. F., and Pérez, F. F.: Anthropogenic carbon distributions in the Atlantic Ocean: data-based estimates from the Arctic to the Antarctic, Biogeosciences, 6, 439–451, 2009, http://www.biogeosciences.net/6/439/2009/. 396, 402

Wallace, D. R.: Storage and transport of excess CO_2 in the oceans: The JGOFS/WOCE Global CO_2 Survey, in *Ocean Circulation and Climate*, 489–521, Elsevier, New York, 2001. 393

Watson, A. J. and Naveira-Garabato, A. C.: The role of Southern Ocean mixing and upwelling in the glacial-interglacial atmospheric CO_2 change, Tellus, 58B, 73–87, doi:10.1111/j.1600-0889.2005.00167.x, 2006. 393

Zickfeld, K., Fyfe, J. C., Saenko, O. A., Eby, M., and Weaver, A. J.: Response of the global carbon cycle to human-induced changes in Southern Hemisphere winds, Geophys. Res. Lett., 34, L12712, doi:10.1029/2006GL028797, 2007. 396, 397

Zickfeld, K., Eby, M., and Weaver, A. J.: Carbon-cycle feedbacks of changes in the Atlantic meridional overturning circulation under future atmospheric CO_2, Global Biogeochem. Cy., 22, GB3024, doi:10.1029/2007GB003118, 2008.

Table 1. List of all performed experiments for the 1850–2099 period. PRE represent preindustrial (i.e., 284.7 ppm) whereas HA2 represents historical and IPCC-A2 emission scenario based atmospheric CO_2 concentration.

Experiment	Climate	CO_2
EXP1	PRE	PRE
EXP2	HA2	HA2
EXP3	HA2	PRE

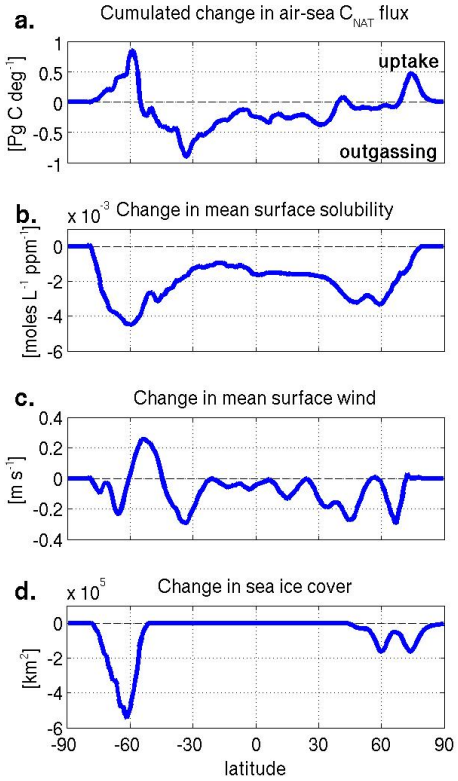

Fig. 1. Latitudinal changes in **(a)** time-integrated air-sea C_{nat} fluxes for the 1850–2099 period, mean difference between EXP1 and EXP3 in **(b)** surface solubility of CO_2, **(c)** mean surface wind speed, and **(d)** sea ice cover computed at the end of the 21st century (2095–2099).

OSD
7, 391–415, 2010

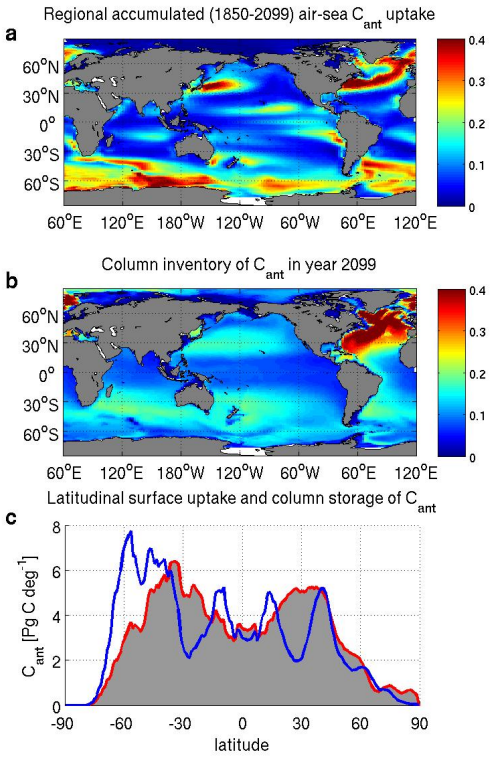

Fig. 2. Spatial distribution of **(a)** accumulated (1850–2099) C_{ant} uptake across the air-sea interface [kmol C m^{-2}], **(b)** column inventory of C_{ant} at the end of experiment period [kmol C m^{-2}], and **(c)** latitudinal distribution of total uptake (blue-line) and storage (grey shading) of C_{ant} [Pg C deg^{-1}].

OSD
7, 391–415, 2010

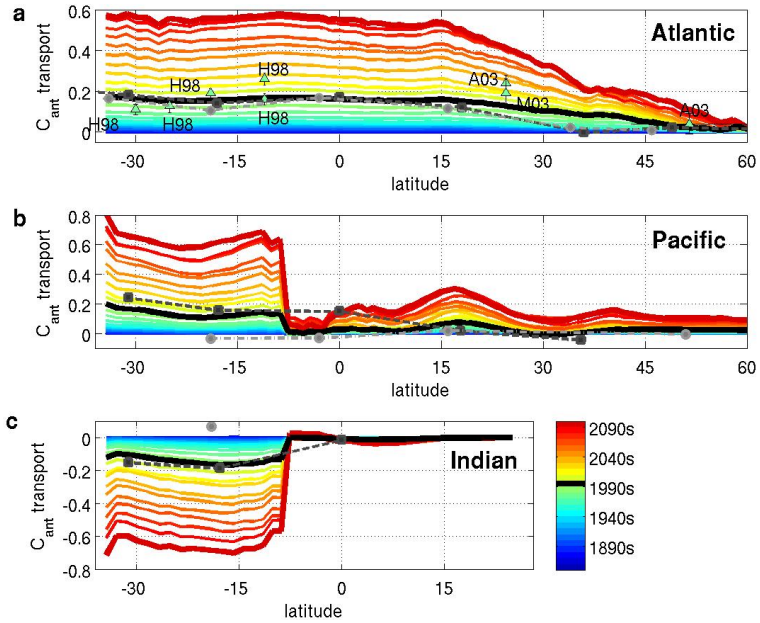

Fig. 3. Simulated meridional transport strength of C_{ant} in the **(a)** Atlantic, **(b)** Pacific, and **(c)** Indian Oceans basin for the 1850–2099 period, plotted as a function of latitude. Each lines represents decadal-averaged northward fluxes. Units are in [Pg C yr^{-1}]. All observations value represent the modern day (1990s–2000s) periods. H98: Holfort et al. (1998), A03: Álvarez et al. (2003), M03: Macdonald et al. (2003), drak grey squares are from inversin study (Mikaloff Fletcher et al., 2006; Gruber et al., 2009), and light grey circles are from mean reconstruction estimates using the Ensemble Kalman Filter(Gerber et al., 2009).

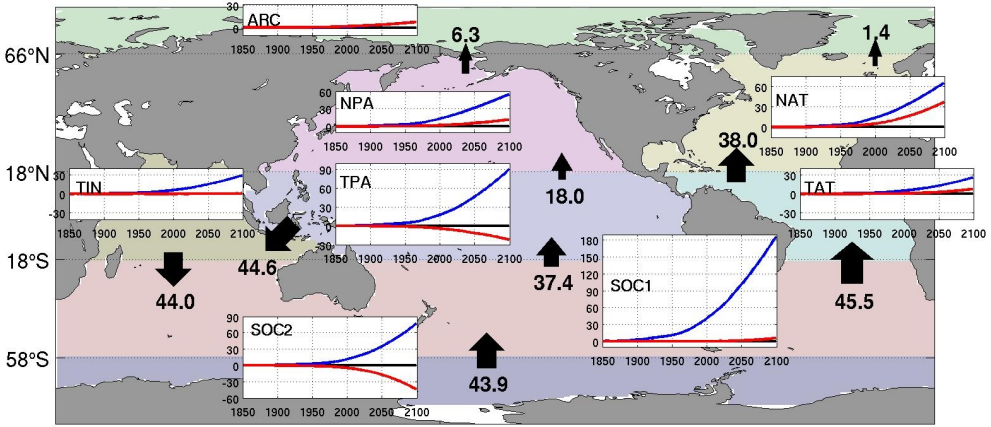

Fig. 4. Accumulated C_{ant} fluxes from the atmosphere (blue-line) as compared to lateral fluxes (red-line) into different ocean regions for the 1850–2099 period. Possitive values represent fluxes into the region and negative otherwise. Regions are defined as follow: Arctic (ARC, >66° N), North Atlantic (NAT, 18° N–66° N), North Pacific (NPA, 18° N–66° N), Tropical Atlantic (TAT, 18° S–18° N), Tropical Pacific (TPA, 18° S–18° N), Tropical Indian (TIN, 18° S–25° N), subtropical Southern Ocean (SOC1, 58° S–18° S), high latitude Southern Ocean (SOC2, >58° S). Arrow and number pairs represent accumulated transport fluxes of C_{ant} between regions for the period 1850–2099. All units are in [Pg C].

OSD
7, 391–415, 2010

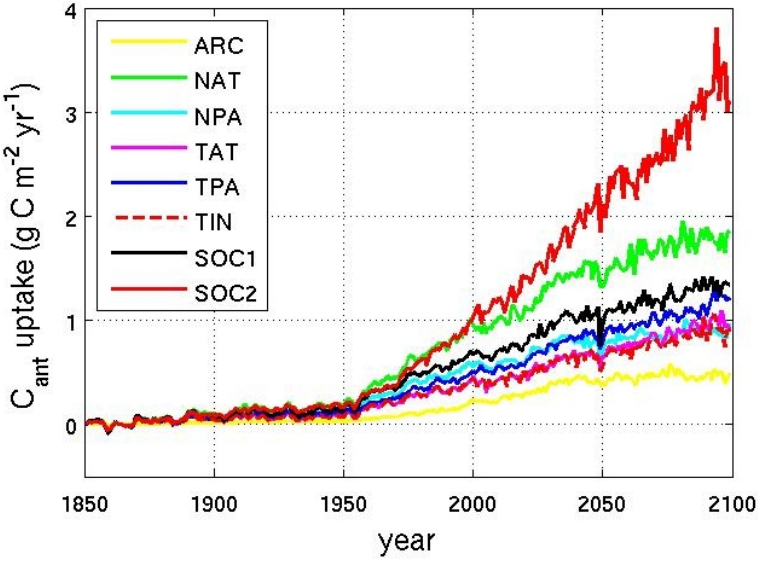

Fig. 5. Time series of area-weighted annual C_{ant} uptake for different ocean regions. Regions definition are similar to that in Fig. 4. Units are in [g C m^{-2} yr^{-1}].